Bioorganic & Medicinal Chemistry Letters 19 (2009) 1686–1690

Contents lists available at ScienceDirect

Bioorganic & Medicinal Chemistry Letters

journal homepage: www.elsevier.com/locate/bmcl

M_3 muscarinic acetylcholine receptor antagonists: SAR and optimization of bi-aryl amines

Brian Budzik [b,*], Yonghui Wang [b,*], Dongchuan Shi [b], Feng Wang [c], Haibo Xie [b], Zehong Wan [a], Chongye Zhu [a], James J. Foley [a], Parvathi Nuthulaganti [c], Lorena A. Kallal [c], Henry M. Sarau [a], Dwight M. Morrow [c], Michael L. Moore [b], Ralph A. Rivero [b], Michael Palovich [a], Michael Salmon [a], Kristen E. Belmonte [a], Dramane I. Laine [a], Jian Jin [a,*]

[a] Centers of Excellence for Drug Discovery, GlaxoSmithKline, 709 Swedeland Road, King of Prussia, PA 19406, USA
[b] Centers of Excellence for Drug Discovery, GlaxoSmithKline, 1250 South Collegeville Road, Collegeville, PA 19426, USA
[c] Molecular Discovery Research, GlaxoSmithKline, 1250 South Collegeville Road, Collegeville, PA 19426, USA

ARTICLE INFO

Article history:
Received 5 December 2008
Revised 29 January 2009
Accepted 29 January 2009
Available online 4 February 2009

Keywords:
Muscarinic acetylcholine receptor
M_3 mAChR
Antagonists
SAR
Sub-type selectivity
COPD
Asthma
Bi-aryl amines

ABSTRACT

Exploration of multiple regions of a bi-aryl amine template led to the identification of highly potent M_3 muscarinic acetylcholine receptor antagonists such as **14** (pA_2 = 11.0) possessing good sub-type selectivity for M_3 over M_2. The structure–activity relationships (SAR) and optimization of the bi-aryl amine series are described.

Five muscarinic acetylcholine receptor (mAChR) sub-types, M_1–M_5, are known to date.[1–3] These seven-transmembrane (7TM) receptors share a common orthosteric ligand-binding site with an extremely high sequence homology, which explains why it has been difficult historically to identify sub-type selective ligands.[3] M_1–M_5 mAChRs are widely distributed in mammalian organs and the central and peripheral nerve system where they mediate important neuronal and autocrine functions.[4,5] In the mammalian lung, only M_1, M_2, and M_3 mAChRs have been recognized as playing important and functional roles.[6] M_3 is predominantly expressed on airway smooth muscle and mediates smooth muscle contraction.[7] M_2 is primarily found on postganglionic nerve termini and functions to limit acetylcholine release from parasympathetic nerves.[8] M_1 is found in parasympathetic ganglia and facilitates neurotransmission through ganglia thus enhancing cholinergic reflexes.[9]

In chronic obstructive pulmonary disease (COPD) and asthma, inflammatory conditions lead to loss of neuronal inhibitory activity mediated by M_2 on parasympathetic nerves, causing excess acetylcholine reflexes[10] which result in airway hyperreactivity and hyperresponsiveness mediated by increased acetylcholine release and thus excess stimulation of M_3. Therefore, potent mAChR antagonists, particularly directed toward the M_3 sub-type, would be useful as therapeutics in these mAChRs-mediated disease states. We previously disclosed a novel muscarinic acetylcholine receptor antagonist bi-phenyl piperazine series, which displayed high potency, good sub-type selectivity for M_3 over M_2, and excellent in vivo efficacy and duration of action.[11] Herein we further describe the structure–activity relationships (SAR) and optimization of this bi-phenyl piperazine series from a high throughput screen (HTS) to the identification of compound **14**.

A HTS of the GSK compound collection identified the bi-phenyl piperazine **1** (Fig. 1),[11] as a M_3 antagonist in a fluorometric imaging

* Corresponding authors at present address: 1031 Perkiomenville Road, Perkiomenville, PA 18074, USA. Tel.: +1 610 754 9132 (B. Budzik); Medicinal Chemistry, R&D China, GlaxoSmithKline, 898 Halei Road, Shanghai 201203, China. Tel.: +1 86 21 61590761; fax: +1 86 21 61590730 (Y. Wang); Center for Integrative Chemical Biology & Drug Discovery, Division of Medicinal Chemistry & Natural Products, Eshelman School of Pharmacy, The University of North Carolina at Chapel Hill, Chapel Hill, NC 27599. Tel.: +1 919 843 8459; fax: +1 919 843 8465 (J. Jin).
E-mail addresses: torqux@yahoo.com (B. Budzik), yonghui.2.wang@gsk.com (Y. Wang), jianjin@unc.edu (J. Jin).

0960-894X/$ - see front matter © 2009 Elsevier Ltd. All rights reserved.
doi:10.1016/j.bmcl.2009.01.098

plate reader (FLIPR) assay[12] with a pIC_{50} of 7.5.[13] On that basis, **1** was considered an acceptable starting point for our lead optimization program aimed at identifying long acting M_3 mAChR antagonists via optimization of their potency.

An efficient and robust solid-phase synthesis permitting modification of several regions of the molecule was developed to explore this series (Scheme 1). Commercially available 3-bromo benzylamines **2** were loaded onto 2,6-dimethoxy-4-polystyrenebenzyloxy benzaldehyde resin (DMHB resin)[14] via reductive amination and coupled with benzoic acids to afford resin-bound aryl bromides **3**. Suzuki coupling of **3** with 3-formylphenyl boronic acids or other formyl substituted aryl boronic acids and subsequent reductive amination of the resulting benzaldehydes with piperazines or various amines, followed by resin cleavage, produced the targeted bi-aryl amines **4** in excellent yields and purity.

We began our initial SAR exploration on the right hand side (RHS) piperazine region of the HTS hit **1** (Table 1).[15] N-Alkylation of the piperazine ring of **1** with methyl (**5a**) or ethyl (**5b**) resulted in over a log unit loss of potency. Replacing the outer piperazine nitrogen with a carbon atom (**5c**) or a non-basic hydrogen bond acceptor as in **5d** yielded poorly active analogs, thus suggesting that a basic center is required for M_3 potency at that position. The homopiperazine analogs **5e** and **5f** did not show improved potency at M_3 compared to the corresponding piperazine derivatives **1** and **5a**. A methylene bridged bicyclic piperazine (**5g**) was nearly equipotent to **1**. The incorporation of a carbonyl group on the methylene linker (**5h**),[16] directly on the piperazine ring to form a lactam (**5i**), or on the terminal nitrogen (**5j**) provided at best poorly active compounds. However, substituting the piperazine with a methyl group (**5k**)[17] enhanced the potency. Further testing of the two stereoisomers of **5k** showed that the (*2S*) enantiomer (**5l**) was the most potent moiety, giving a potency increase of 0.8 log unit over **1**. An attempt was also made to introduce a quaternary ammonium moiety to the molecule in order to reduce cell membrane permeability. However, these efforts were fruitless as quaternizing either the inner nitrogen (**5n**)[18] or the outer nitrogen (**5o**)[19] did not maintain potency.

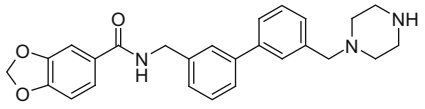

1, M_3 FLIPR pIC_{50} = 7.5

Figure 1. In vitro profile of HTS hit **1**.

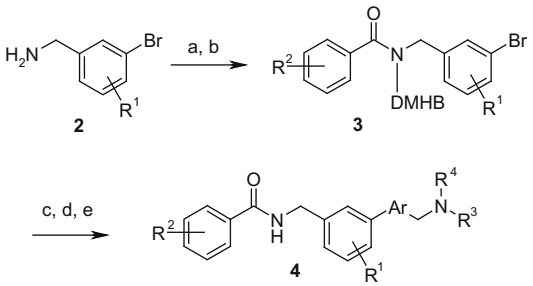

Scheme 1. Reagents and conditions: (a) DMHB resin, $Na(OAc)_3BH$, DIEA, 10% AcOH in NMP, rt; (b) various benzoic acids, DIC, NMP, rt; (c) various 3-formylphenyl boronic acids or other formyl substituted boronic acids, $Pd(PPh_3)_4$, 2 M Cs_2CO_3, DME, 80 °C; (d) piperazines or various amines, $Na(OAc)_3BH$, Na_2SO_4, DCE, rt; (e) 50% of TFA in DCE, rt.

Generally, modification of the RHS phenyl ring did not improve potency (Table 2). Thus, introduction of substituents onto the phe-

Table 1
SAR of the RHS diamine region

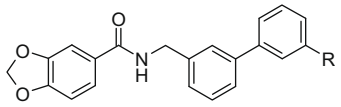

Compound	R	M_3 pIC_{50}
1	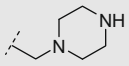	7.5
5a	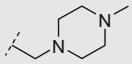	6.3
5b	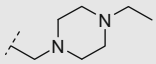	5.8
5c	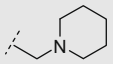	5.2
5d	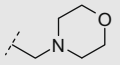	<5.0
5e	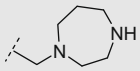	6.5
5f	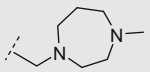	6.2
5g	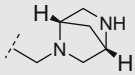	7.1
5h	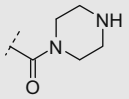	5.3
5i	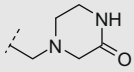	<5.0
5j	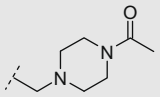	5.4
5k	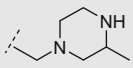	8.0
5l	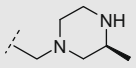	8.3
5m	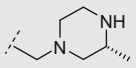	7.3
5n	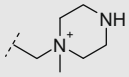	<5.0
5o	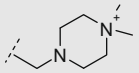	5.6

nyl ring, gave compounds (**6a**, **6b**, and **6c**) of lower potency than **1**. A similar outcome was observed when the phenyl ring was replaced with a pyridine (**6d**) or a thiophene (**6e**).

The left hand side (LHS) phenyl ring of the bi-aryl, in contrast, proved to be another potency enhancing region (Table 3). The addition of fluorine at position 6 of the LHS phenyl ring (**7a**) improved the potency to a pIC_{50} of 8.2. Incorporation of a methoxy group at the same position (**7b**) gave an equipotent compound to **1**, while other substitutions resulted in potency losses (**7c**–**7f**).

In the amide linker region, replacement of the amide group of **1** (Table 4) with a sulfonamide (**8a**)[20] led to a 10-fold loss of potency. Removal of the methylene (**8b**)[20] or replacement of the amide with a urea (**8c**)[20] resulted in even greater potency decrease at M_3.

The attachment point and nature of various substituents on the LHS benzamide phenyl were subsequently explored in a systematic manner (Table 5). An initial set of compounds, investigating various electron-donating and electron-withdrawing groups of different sizes (**9a–9l**), clearly established that the 3- or *meta*-position was the most preferred but did not uncover any compound more potent than **1**.

Building on this finding, our next step was to focus exclusively on the *meta*-position and investigate a larger set of substituents (**9m–9z**). From this exercise, the acetyl **9v** and ethoxy **9t** stood out, both displaying a M_3 pIC_{50} of 8.0. The most promising result, however, was the identification of the *N*-methyl piperazine derivative **9z**. In addition to being the most potent of the *meta* derivatives prepared, it also showed that amine containing

Table 2
SAR of the bi-aryl RHS phenyl ring

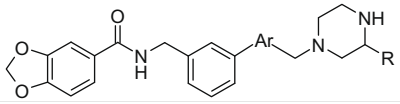

Compound	Ar	R	M_3 pIC_{50}
1	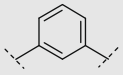	H	7.5
6a	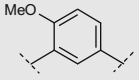	H	5.9
6b	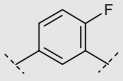	H	6.7
6c	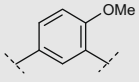	H	6.5
5l	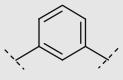	(*S*)-Methyl	8.3
6d	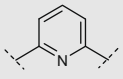	(*S*)-Methyl	7.4
6e	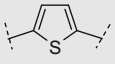	(*S*)-Methyl	6.3

Table 3
SAR around the bi-aryl LHS phenyl ring

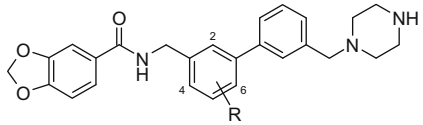

Compound	R	M_3 pIC_{50}
1	6-H	7.5
7a	6-F	8.2
7b	6-OMe	7.5
7c	4-F	6.6
7d	4-Me	5.5
7e	2-F	5.6
7f	2-Me	<5.0

Table 4
SAR of the amide linker region

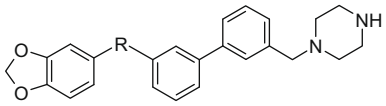

Compound	R	M_3 pIC_{50}
1	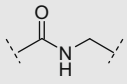	7.5
8a	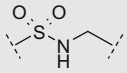	6.6
8b	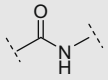	5.2
8c	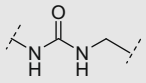	5.1

Table 5
SAR of the monosubstituted benzamides

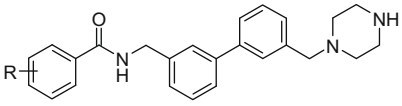

Compound	R	M_3 pIC_{50}
9a	2-CN	6.5
9b	3-CN	7.3
9c	4-CN	7.1
9d	2-OMe	6.3
9e	3-OMe	7.1
9f	4-OMe	6.3
9g	2-Cl	6.0
9h	3-Cl	7.0
9i	4-Cl	6.5
9j	2-CF_3	5.4
9k	3-CF_3	7.3
9l	4-CF_3	6.2
9m	3-F	6.1
9n	3-COOMe	7.7
9o	3-SO_2Me	7.7
9p	3-$N(CH_3)_2$	6.7
9q	3-NH_2	5.7
9r	3-NHAc	6.7
9s	3-OCF_3	6.3
9t	3-OEt	8.0
9u	3-OPh	5.9
9v	3-Ac	8.0
9w	3-OH	5.7
9x	3-Me	6.6
9y	3-Et	6.5
9z	3-*N*-Methyl piperazin-methyl	8.4

functionalities could be placed on the LHS, thus introducing new potential quaternization points into the template.

Encouraged by the good potency of **9z**, we proceeded to explore the SAR around its key *N*-methyl piperazine moiety. At that stage, it was also decided to incorporate the previously identified potency enhancing modifications, the (2*S*)-2-methyl piperazine group of **5l** and the fluoro substituent of **7a**, into the core template. To enable this study, we needed first to modify our existing solid-phase route to make it amenable to the introduction of diverse amines/diamines or quaternized amines/diamines on the LHS (Scheme 2). 3-Bromo-4-fluorobenzylamine **10** was loaded onto a DMHB resin via reductive amination, followed by coupling with 3-formylphenyl benzoic acid and subsequent reductive amination with various amines or diamines, leading to resin-bound benzylamines **11**. Subsequent Suzuki coupling of **11** with 3-formylphenyl boronic acid followed by reductive amination with (2*S*)-2-methyl piperazine and resin cleavage, produced the targeted bi-phenyl piperazines **12**. An optional quaternization step after Suzuki coupling using methyl iodide or various alkyl halides gave quaternized bi-phenyl piperazines such as **13a** and **13b**.

The results of the SAR investigation of the LHS amine region are shown in Table 6. The piperazine derivatives **12a**, **12b**, and **12c** showed improved M_3 activity with respective pA_2 values[21] of 9.8, 10.5, and 10.2. Gratifyingly, the M_3 potency of the *N*-methylpiperazine **12b** increased over 2 log units compared to the analogous **9z**, indicating the potency enhancements installed in each region of **12b** (compare with **5l** and **7a**) were additive. The M_3 potencies of *N*-methylhomopiperazine **12d** and the acyclic methylated diamine **12e** were similar to **12a**. Monoamines were also tolerated in the region. Thus, formamide **12f** and morpholine **12g** showed excellent M_3 potency. The piperidine **12h** and the simple dimethyl amine

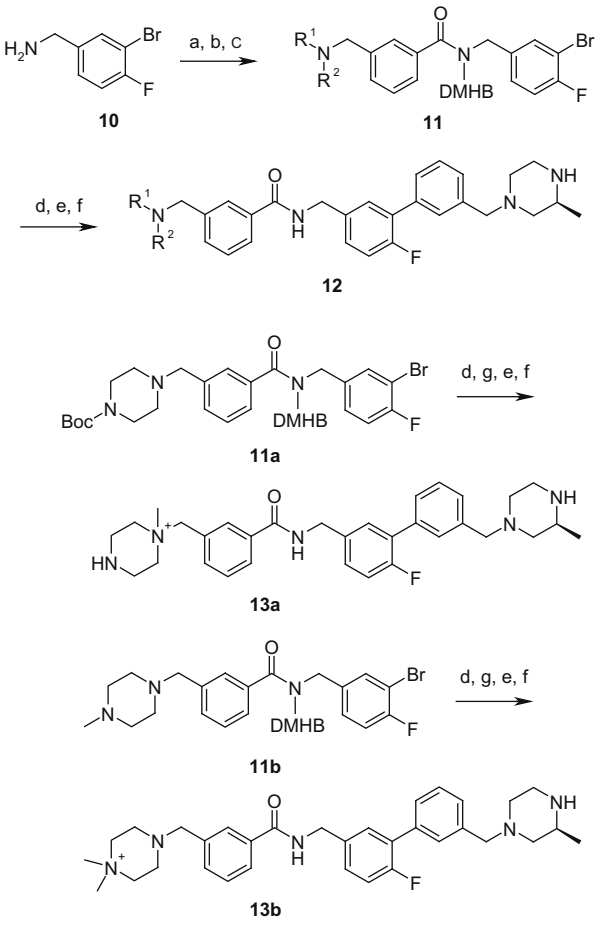

Scheme 2. Reagents and conditions: (a) DMHB-resin, $Na(OAc)_3BH$, DIEA, 10% AcOH in NMP, rt; (b) 3-formyl benzoic acid, DIC, DCE/DMF 1:1, rt; (c) R^1R^2NH, $Na(OAc)_3BH$, Na_2SO_4, DCE, rt; (d) 3-formylphenyl boronic acid, $Pd(PPh_3)_4$, 2 M Cs_2CO_3, DME, 80 °C; (e) (2*S*)-2-methylpiperazine, $Na(OAc)_3BH$, Na_2SO_4, DCE, rt; (f) 50% of TFA in DCE, rt; (g) MeI, CH_3CN, rt.

Table 6
SAR of the LHS amine region

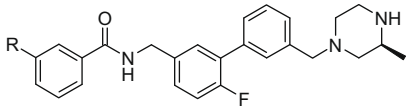

Compound	R	M_3 pA_2
12a	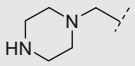	9.8
12b	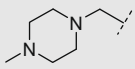	10.5
12c	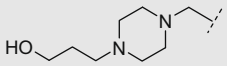	10.2
12d	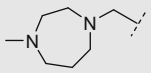	9.6
12e	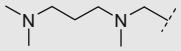	9.7
12f	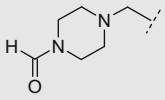	10.1
12g	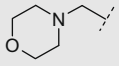	9.9
12h	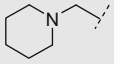	9.2
12i		8.5
13a	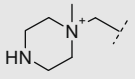	8.5
13b	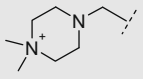	9.8
13c	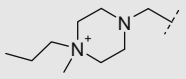	10.0
13d	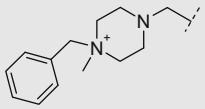	10.1
13e	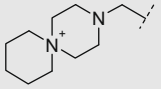	9.9
14	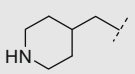	11.0

12i showed decreased potency compared to **12a**–**12g**, suggesting that an outlying heteroatom may be needed for maximum M_3 potency.

Unlike the RHS diamine region, quaternization was well tolerated in the LHS diamine region (Table 6). Quaternization of the outer nitrogen of **12a** was more favored than that of the inner nitrogen (**13a**) and led to a compound **13b**, which was equipotent to **12a**. Other quaternized piperazines (**13c–13e**) also gave excellent M_3 potencies with pA_2 values around 10. Quaternary ammonium salts such as **13b** indeed had extremely low membrane permeability (<3 nm/s).[22] Interestingly, the increased basicity of the piperidine derivative **14** compared to **12a**,[23] correlated with an increased affinity for the M_3 receptor, suggesting that the terminal N of these molecules may be interacting with an acidic residue. As previously reported, compound **14** was found to exhibit sub-type selectivity for M_3 over M_1 and M_2 (pA_2s for M_3, M_2, and M_1 are 11.0, 8.3, and 9.7, respectively).[11] In addition, **14** also displayed excellent inhibitory activity and long duration of action in a bronchoconstriction in vivo model via intranasal administration.[11]

In summary, the extensive SAR exploration of multiple regions of the HTS hit **1** led to the identification of key structural motifs necessary to achieve high M_3 potency. The combination of these features resulted in the discovery of the highly potent M_3 antagonist **14** (pA_2 = 11.0).

Acknowledgments

We thank Bing Wang for NMR, Qian Jin for LC/MS, Carl Bennett for purification, and Christina Schulz-Pritchard, Jim Fornwald, and Jeffrey Guss for assay support.

References and notes

1. Caulfield, M. P.; Birdsall, N. J. M. *Pharmacol. Rev.* **1998**, *50*, 279.
2. Eglen, R. M. *Prog. Med. Chem.* **2005**, *43*, 105.
3. Hulmes, E. C.; Birdsall, N. J. M.; Buckley, N. J. *Ann. Rev. Pharmacol. Toxicol.* **1990**, *30*, 633.
4. Caulfield, M. P. *Pharmacol. Ther.* **1993**, *58*, 319.
5. Eglen, R. M. *Auto. Autacoid Pharmacol.* **2006**, *26*, 219.
6. Lee, A. M.; Jacoby, D. B.; Fryer, A. D. *Curr. Opin. Pharmacol.* **2001**, *1*, 223.
7. (a) Barnes, P. J. *Thorax* **1989**, *44*, 161; (b) Gater, P. R.; Alabastar, V. A.; Piper, I. *Pulm. Pharmacol.* **1989**, *2*, 87.
8. Faulkner, D.; Fryer, A. D.; MacLagan, J. *Br. J. Pharmacol.* **1986**, *88*, 181.
9. Lammers, J. W. J.; Minnette, P. A.; Mc Custer, M.; Barnes, P. J. *Annu. Rev. Respir. Dis.* **1989**, *139*, 446.
10. Fryer, A. D.; Adamko, D. J.; Yost, B. L.; Jacoby, D. B. *Life Sci.* **1999**, *64*, 449.
11. Jin, J.; Budzik, B.; Wang, Y.; Shi, D.; Wang, F.; Xie, H.; Wan, Z.; Zhu, C.; Foley, J. J.; Webb, E. F.; Berlanga, M.; Burman, M.; Sarau, H. M.; Morrow, D. M.; Moore, M. L.; Rivero, R. A.; Palovich, M.; Salmon, M.; Belmonte, K. E.; Lainé, D. I. *J. Med. Chem.* **2008**, *51*, 5915.
12. (a) Measuring inhibition of acetylcholine-mediated $[Ca^{2+}]_i$-mobilization in Chinese hamster ovary (CHO) cells stably expressing human recombinant M_3 receptor.; (b) For FLIPR assay details, see supporting information in Ref. 11.
13. The biological assay results in the paper are a mean of at least 2 determinations with standard deviation of <±0.3, and data for compounds M_3 $pIC_{50} > 7.0$ are from 96-well FLIPR assay, <7.0 from 384 well FLIPR assay, unless otherwise noted.
14. (a) Jin, J.; Graybill, T. L.; Wang, M. A.; Davis, L. D.; Moore, M. L. *J. Comb. Chem.* **2001**, *3*, 97; (b) Available from Polymer Laboratories, Part number: 1466-6689, 150–300 μm, 1.5 mmol/g loading.
15. (a) All new compounds in this paper were characterized via LC/MS and ^1H NMR.; (b) For representative experimental procedures, see supporting information in Ref. 11.
16. Compound **5h** was synthesized by using 3-(dihydroxyboranyl)benzoic acid instead of 3-formylphenyl boronic acid in step (c) of Scheme 1, followed by DIC mediated coupling with Boc-piperazine, followed by cleavage step (e).
17. Use of any unprotected, 2-substituted piperazine in step (d) of Scheme 1 gives completely selective reductive amination at the less hindered nitrogen.
18. Quaternization of the inner piperazine nitrogen in **5n** was affected by use of Boc-piperazine in step (d) of Scheme 1, followed by reaction of the washed resin with excess CH_3I in CH_3CN at rt for overnight, followed by cleavage step (e).
19. Quaternization of the outer piperazine nitrogen in **5o** was affected by use of *N*-methyl-piperazine in step (d) of Scheme 1, followed by reaction of the washed resin with excess CH_3I in CH_3CN at rt for overnight, followed by cleavage step (e), quaternization being completely selective for the less sterically hindered outer nitrogen.
20. Compounds **8a** and **8c** were prepared by performing sulfonylation (using 1,3-benzodioxole-5-sulfonyl chloride in presence of DMAP in pyridine/DCE), or urea formation (using 5-isocyanato-1,3-benzodioxole in DCE), respectively, instead of amide formation in step (b) of Scheme 1. Compound **8b** was prepared by using 3-bromoaniline instead of 3-bromobenzylamine in step (a) of Scheme 1, and required more forcing amide coupling conditions in step (b): DMAP, DIC, in DCE/DMF at 80 °C.
21. The pIC_{50} limit of the M_3 FLIPR assay was about 9.0. pA_2 was determined and used to compare potency for compounds with pIC_{50} reaching the limit. See Ref. 11 for assay details of pA_2 determination.
22. The artificial phospholipid membrane technique is similar to the widely used Caco-2 cell monolayer permeation technique. In short, egg phosphatidyl choline (1.8%) and cholesterol (1%) are dissolved in *n*-decane. A small amount of the volatile mixture is applied to the bottom of the microfiltration filter inserts. Phosphate buffer (0.05 M, pH 7.05) is quickly added to the donors and receivers, and the lipids are allowed to form self-assembled lipid bilayers across the small holes in the filter. Permeation experiment is initiated by spiking the compounds of interest to the donor sides, and the experiment is stopped at a pre-determined elapsed time. The samples are withdrawn and transferred to appropriate vials for analysis by HPLC with UV detection (215 nm).
23. Full experimental procedures and characterization for the synthesis of piperidine **14** are given in Ref. 11.